The Nature of Variations of Ammonia Proton Affinity in an Argon Environment

Jaroslaw J. Szymczak,[†,‡] Jan Urban,[†,§] Szczepan Roszak,[†,‡] and Jerzy Leszczynski*[,†]

Computational Center for Molecular Structure and Interactions, Department of Chemistry, Jackson State University, P.O. Box 17910, Jackson, Mississippi 39217, Institute of Physical and Theoretical Chemistry, Wroclaw University of Technology, Wybrzeze Wyspianskiego 27 50-370 Wroclaw, Poland, and Department of Biophysics and Chemical Physics, Faculty of Mathematics, Physics, and Informatics, Comenius University, Mlynska Dolina F1, 84248 Bratislava, Slovakia

Received: December 8, 2005; In Final Form: September 23, 2006

The presence of solvent molecules, even inert, may significantly influence processes taking place in the gas phase. The reason for the solvent activity may be found in studies of complexes originating from microsolvation. The structure, thermodynamics, and vibrational properties of $NH_4^+Ar_n$ ($n = 0-5$) and NH_3Ar_n ($n = 0-4$) complexes are presented in this work with the aim to elucidate the effect of microsolvation on protonation/deprotonation processes. The relation between the nature of interactions in cationic and neutral clusters and the proton affinity is studied as a function of the number of ligands in complexes.

I. Introduction

The gas-phase processes are sensitive to the presence of solvent molecules. The above also is true when the solvent is constituted by inert species such as noble atom gases. The process of argon-catalyzed proton transfer was observed and characterized for the HOC^+ to HCO^+ rearrangement.[1] The experiments provide systematic data on clustering of the moieties of interest with solvent atoms and molecules. Three main sources of information on clusters in the gas phase are mass,[2] photoelectron,[3] and infrared spectroscopies.[4] The results of experiments are often complex and provide only a fraction of information required to deduce the mechanisms of the observed processes. The theoretical studies, calibrated by the reproduction of available experimental data, supplement measurements and allow for the systematic characterization of properties of the investigated species and for removing often present ambiguities. The influence of clustering has been studied for molecular properties such as electron affinity[5] and ionization.[6] The proton attachment/detachment processes in the gas-phase environment are interesting as precursors of many proton-transfer reactions observed in nature. The interactions of the NH_4^+ cation with inert molecules or atoms have been studied quite extensively. However, even the molecular structure of the smallest complex, NH_4^+He, was disputed[7,8] because its infrared (IR) spectra do not provide a definitive answer regarding its geometry. The question of vertex vs face-bound global minimum also was raised for NH_4^+ complexes solvated by Ne, Ar, and H_2.[9,10] Theoretical studies are needed to provide a convincing elucidation of the above ambiguity.

The complexes of NH_4^+ with argon atoms were studied by means of infrared photodissociation spectroscopy. Most often studies were performed for the single argon complex, although a study of extended complexes (for the number of atoms up to 7) also was carried out.[11,12] The experimental data for $NH_4^+Ar_n$ ($n > 1$) were complemented by restricted Hartree−Fock calculations; however, their interpretation should be treated with caution. The investigation of molecular NH_3Ar_n complexes are restricted to NH_3Ar, which was studied both experimentally[13−15] and theoretically.[16,17]

In the presented work, we report the properties of cationic $NH_4^+Ar_n$ and neutral NH_3Ar_n ($n = 0-5$) complexes as components of protonation/deprotonation processes. The variation of proton affinity as a function of consecutive argon attachment is also investigated. The nature of the above property is studied in connection with an analysis of interaction energy decomposition components performed for charged and neutral complexes. The investigation of vibrational frequencies variation was performed for the $NH_4^+Ar_n$ deprotonation process.

II. Theoretical Methods

The optimal molecular structures and harmonic vibrational frequencies of the studied clusters were determined by means of the second-order Møller−Plesset perturbation theory (MP2)[18] applying the extended aug-cc-pVTZ basis set.[19−21] All electrons were correlated in performed calculations. The geometry optimizations were performed utilizing the standard supermolecular technique.[22] Interacting complexes also were optimized applying potential energy surfaces that were corrected for the basis set superposition error using the Boys−Bernardi counterpoise (CP) scheme.[23,24] In the second approach, the ammonia part and each of the argon atoms were constituting interacting fragments. The MP2 calculations lead to the electron polarizability of Ar of 10.88 a_o^3, which is close to the experimental value (11.08 a_o^3).[25] The proper reproduction of polarizability ensures the reasonable representation of the dispersion interaction energy by the applied level of theory. The Ar_2 dissociation energy corrected for the basis set superposition error and its separation distances calculated at the MP2/aug-cc-pVTZ level are 0.39 kcal/mol and 3.681 Å (uncorrected) and 0.20 kcal/mol and 3.839 Å (CP-corrected). The coupled cluster method with single and double substitutions and noniterative triple excitiations [CCSD(T)] in the same basis set gives 0.34 kcal/mol and 3.724 Å (uncorrected) and 0.18 kcal/mol and 3.890 Å

* Corresponding author. E-mail: jerzy@ccmsi.us.
† Jackson State University.
‡ Wroclaw University of Technology.
§ Comenius University.

10.1021/jp057166c CCC: $33.50
Published on Web 11/09/2006

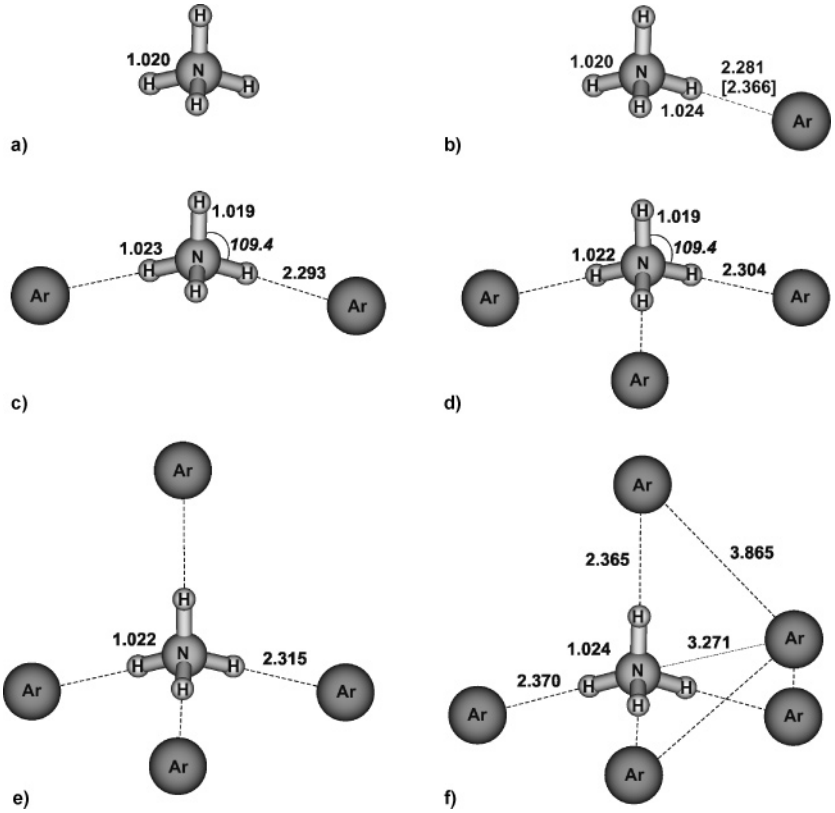

Figure 1. (a−f) The ground-state complexes of $NH_4^+Ar_n$ ($n = 0-5$) resulting from standard and supermolecular optimization. The parameters for NH_4^+Ar from CP-corrected optimization are given in square brackets. Distances in angstroms, angles in degrees.

(CP-corrected), respectively. The comparison with measured values[26] of 0.283 kcal/mol and 3.761 Å indicates that the experimental value is confined by applied approaches with the CP-corrected distance being always longer. The calibration allows for a confidence in the overall predictions of structures and energetics of the studied complexes. The single point calculations at the CCSD(T)[27,28] was further applied to enhance the quality of the theoretical dissociation energies. The vibrational properties were calculated applying the harmonic oscillator approximation.[29] The electron distribution was studied using the natural bond orbital (NBO)[30] electronic population analyses approach and the MP2 electron densities.

The intermolecular interactions were studied using the hybrid variational−perturbational interaction energy decomposition scheme.[31−33] In this approach, the Hartree−Fock interaction energy is partitioned

$$\Delta E^{HF} = \epsilon_{el}^{(10)} + \epsilon_{ex}^{HL} + \Delta E_{del}^{HF} \quad (1)$$

into first-order electrostatic $\epsilon_{el}^{(10)}$, Heitler-London exchange ϵ_{ex}^{HL}, and the higher order delocalization energy ΔE_{del}^{HF} terms. The electron correlation effects are taken into account by means of the Møller−Plesset perturbation theory. The $\epsilon_{MP}^{(2)}$ interaction energy, which includes the dispersion contribution and correlation corrections to the Hartree−Fock components, is calculated in the supermolecular approach

$$\epsilon_{MP}^{(2)} = E_{AB}^{(2)} - E_{A}^{(2)} - E_{B}^{(2)} \quad (2)$$

All interaction energy terms are calculated consistently in the dimer-centered basis set and therefore are free from the basis set superposition error due to the full counterpoise correction.[24,34]

Calculations of the equilibrium geometries and normal frequency analysis have been performed using the Gaussian 03 suite of codes.[35] The interaction energy decomposition scheme was implemented[36] in the Gamess program.[37]

III. Results and Discussion

A. Structure and Energetics of Ionic and Neutral Dimers. The available experimental data do not provide a definitive answer to whether the global minimum structure corresponds to the one with Ar atoms bound to the vertexes or faces of the NH_4^+ tetrahedron.[11] On the basis of the results of ab initio calculations, the vertex-bound structures were predicted for the sequence of $NH_4^+Ar_n$ ($n = 1-4$) complexes.[12] The predictions for $n > 2$ were based on the Hartree−Fock level, which may not be adequate for complexes including noble gases. However, calculations accounting for the correlation energy (MP2), performed in this work, confirm the former predictions. Both optimization approaches involving potential energy surface of NH_4^+Ar (corrected and not-corrected for the basis set superposition error) lead to similar structural parameters (Figure 1). The H−Ar distance predicted applying CP-correction is 0.08 Å longer from the standard supermolecule optimization. Taking into account the tendency of the CP-correction to overestimate distances,[38] the results of both approaches are of the similar quality. The further reported and discussed structures of $NH_4^+Ar_n$ were deduced by applying standard supermolecule optimization. The vertex-bound structures predicted by ab initio optimizations for the NH_4^+He and $NH_4^+(H_2)_n$ ($n = 1-4$) complexes[10,39] indicate that such binding represents a more general structural feature. The proper location of the structures is indirectly confirmed by the reproduction of estimated experimental values of dissociation energies (Table 1) and splittings of the ν_3 fundamental mode. The calculated splittings

TABLE 1: The Consecutive Dissociation Energies of $NH_4^+Ar_n$ and NH_3Ar_n Complexes Calculated at the MP2 and CCSD(T) Levels of Theory. Energies in kcal/mol.

	shell	D_e MP2	D_e(BSSE) MP2	D_e CCSD(T)	D_o MP2	D_o(BSSE) MP2	D_o exper
				$NH_4^+Ar_n$			
NH_4^+Ar	A(1)	3.90	2.59	3.92	3.15	1.84	2.36[b]
NH_4^+Ar[a]	A(1)	3.83	2.64	3.85	3.37	2.18	2.36[b]
$NH_4^+Ar_2$	A(2)	3.77	2.46	3.77	3.21	1.90	
$NH_4^+Ar_3$	A(3)	3.67	2.34	3.67	3.24	1.91	
$NH_4^+Ar_4$	A(4)	3.60	2.24	3.60	3.23	1.87	
$NH_4^+Ar_5$	A(4)B(1)[f]	2.74					
				NH_3Ar_n			
NH_3Ar[a]	A(1)	0.71	0.37	0.69	0.48	0.14	0.43[c] 0.33[d] 0.38[e]
NH_3Ar_2[a]	A(2)	1.08	0.55	1.02	0.93	0.40	
NH_3Ar_3[a]	A(3)	1.46	0.76	1.36	1.35	0.67	
NH_3Ar_4[a]	A(3) B(1)	1.35	0.78		1.24	0.67	

[a] Geometry of complexes from optimization based on CP-corrected potential energy surface. [b] Reference 8. [c] Reference 15. [d] Reference 16. [e] Reference 17. [f] The MP2 level based on the frozen core approximation.

(56, 80, 54 cm^{-1} for $n = 1, 2, 3$) reasonably reproduce the corresponding experimental values (43, 70, 48 cm^{-1}) despite the rather harsh approximations applied for the frequency calculations. Interestingly, the stable "face" bond isomer also was located but is higher in energy by 1.2 kcal/mol (0.59 kcal/mol when counterpoise corrected).

The consecutive attachment of ligands slightly weakens the H^+-Ar bonds leading to longer H^+-Ar distances and lower sequential dissociation energies (Table 1). The increase of the cluster size beyond four Ar atoms proceeds through the symmetrical face attachment. The energetically favored $NH_4^+Ar_5$ structure is due to the direct N−Ar bonding with an interatomic distance of 3.27 Å, which is shorter than the average $N-H^+-Ar$ bond (3.39 Å). The interactions with the other ligands lead to the most symmetrical structure (C_{3v}). The distances between the face-bound ligand and vertex-bound argons are similar to the one observed in the Ar_2 dimer. The second shell is characterized by the significantly smaller interaction energies.

The deprotonation of $NH_4^+Ar_n$ ($n = 1-4$) leads to significantly less stable neutral species where NH−Ar and Ar−Ar interactions are energetically comparable. The weak interactions are sensitive to the effect of basis set superposition error, and the potential surface, which is not CP-corrected, may no longer be adequate to describe such complexes. Two isomers of NH_3Ar were found to be very close in energy. The structure proposed as a result of spectroscopic investigations[15] possesses C_s symmetry with an Ar atom attached to two hydrogen atoms (Figure 1a). This type of a structure also results from CP-corrected potential energy surface (PES) optimization performed in this work as well as from other available theoretical studies.[16,17] The second isomer, however, was found to be only 0.09 kcal/mol higher in energy (CP-corrected) and also has to be considered as a candidate for the ground state. However, standard supermolecular optimization results in an isomer with an Ar atom attached to the single hydrogen atom (Figure 1b). The isomer with two hydrogens bonded to Ar is characterized by an N−Ar distance of 3.618 Å, which is 0.48 Å longer from the spectroscopically determined value. The calculated distance in the standard optimization is shorter by 0.11 Å than the experimental bond length. The results suggest that the CP-corrected method overestimates distances while the standard supermolecular approach leads to the underestimation of distances. The angle between the N−Ar vector and the approximate C_{3v} axis of NH_3 (90.3 degrees) reasonably agrees with the experimental value (96.6 degrees). The calculated dissociation energies are in good agreement with the experimental values (Table 1) The third isomer determined characterized by three NH−Ar bonds (C_{3v}) is within 0.2 kcal/mol of the ground-state isomer. The calculations indicate a flat potential surface allowing for dynamical complex with NH_3 rotations. Interestingly, the optimization without CP-correction favors the single NH−Ar bonded structure.

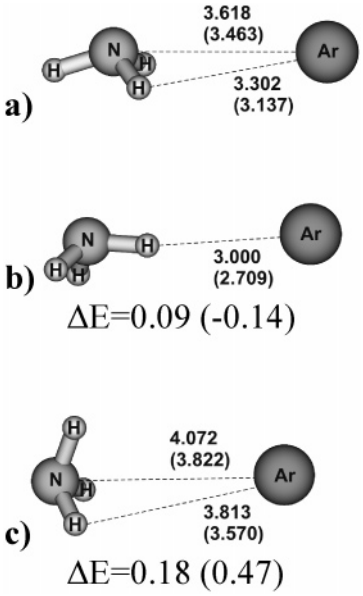

Figure 2. (a−c) The energetically lowest isomers of NH_3Ar from CP-corrected and standard (in parentheses) optimizations. Distances in angstroms, angles in degrees, energies in kcal/mol.

The addition of Ar to the NH_3Ar complex leads to the structure presented in Figure 3 as characterized by one Ar interacting with two NH hydrogens (in analogy to the NH_3Ar ground state), and the second Ar forming the NH−Ar bond in the plane of three atoms (in analogy to the second energetically lowest isomer of NH_3Ar). This arrangement allows Ar−Ar interactions to reproduce the distance of the argon dimer. A number of isomers higher in energy also was located including the isomer in which two Ar atoms interact with the same pair of NH (Figure 3b). The isomer possessing separated Ar atoms also exists (Figure 3c).

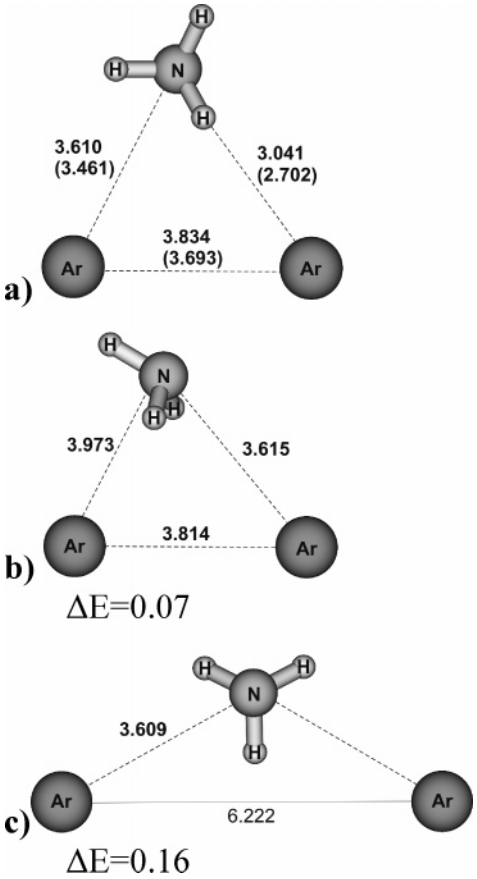

Figure 3. (a−c) The energetically lowest isomers of NH_3Ar_2 from CP-corrected and standard (in parentheses) optimizations. Distances in angstroms, angles in degrees, energies in kcal/mol.

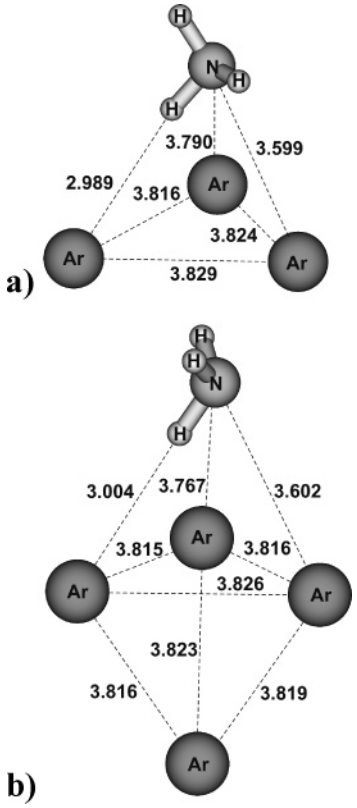

Figure 4. The energetically lowest isomers of NH_3Ar_3 (a) and NH_3Ar_4 (b) from CP-corrected. Distances in angstroms, angles in degrees.

The NH_3Ar_3 complex is represented by a tetrahedral structure (Figure 4a) with bonds satisfying the optimal N−Ar and Ar−Ar distances. A number of other stable structures have been found that are characterized by an Ar_3 triangle and NH_3 in the corner of the tetrahedron. However, these structures are higher in energy by more then 0.24 kcal/mol. The NH_3Ar_4 molecule possesses a geometry of trigonal bipyramid (Figure 4b). The NH_3Ar_n ($n = 1-4$) complexes are formed in analogy to Ar_n complexes[40] with one Ar atom being replaced by an ammonia molecule. The energetically close isomers represent complexes with a different arrangement of NH_3 with regard to the Ar network. The Cartesian coordinates of the studied complexes are supplied as Supporting Information.

B. The Nature of Interactions in Cationic and Neutral Complexes. Though the molecular structures of many cationic and neutral complexes are similar, the nature of their interactions is significantly different. The consecutive interaction energies in ($NH_4^+Ar_{n-1}$−Ar) cations result mainly from the cancellation of the exchange and delocalization terms. The electrostatic and correlation contributions are smaller and depend weakly on the size of clusters. The variation of total consecutive interaction energies is governed by the difference between exchange and delocalization contributions (Table 2). The resulting total consecutive interaction energies contain approximately constant contribution from the sum of electrostatic and correlation interactions and the variable part that is due to the exchange and delocalization terms. The consecutive total interaction energy is almost a linear function of the size of the cluster. Despite the large Ar−Ar separation in the NH_4^+Ar−Ar complex (Figure 1c) the three-body contribution to the total interaction energy amounts to almost four percent (Table 3). The three-body interactions are dominated by the large contribution of the delocalization energy. The extended cancellation of the two-body ϵ_{ex}^{HL} and ΔE_{del}^{HF} terms emphasize the importance of three-body interactions amounting to as much as 11% of the total

TABLE 2: The Interaction Energy Decomposition Terms for the $NH_4^+Ar_{n-1}\cdots Ar$ and $NH_3Ar_{n-1}\cdots Ar$ Systems. Values in kcal/mol.

interacting system	$\epsilon_{el}^{(10)}$	ϵ_{ex}^{HL}	ΔE_{del}^{HF}	ΔE_{HF}	$\epsilon_{disp}^{(2)}$	$\epsilon_{MP}^{(2)}$	ΔE_{tot}
$NH_4^+\cdots Ar$	−0.554	3.917	−4.204	−0.840	−1.754	−1.812	−2.652
$NH_4^+\cdots Ar^a$	−0.257	2.839	−3.449	−0.866	−1.221	−1.207	−2.073
$NH_4^+Ar\cdots Ar$	−0.546	3.784	−3.934	−0.696	−1.780	−1.815	−2.511
$NH_4^+Ar_2\cdots Ar$	−0.539	3.664	−3.696	−0.571	−1.804	−1.821	−2.392
$NH_4^+Ar_3\cdots Ar$	−0.532	3.555	−3.485	−0.462	−1.828	−1.828	−2.291
$NH_3\cdots Ar^a$	−0.133	0.466	−0.050	0.283	−0.745	−0.658	−0.374
$NH_3Ar\cdots Ar^a$	−0.188	0.700	−0.077	0.434	−1.101	−0.990	−0.556
$NH_3Ar_2\cdots Ar^a$	−0.309	1.004	−0.102	0.593	−1.575	−1.373	−0.780
$NH_3Ar_3\cdots Ar^a$	−0.279	0.947	−0.044	0.624	−1.564	−1.404	−0.780

[a] Geometry of complexes from optimization based on CP-corrected potential energy surface.

TABLE 3: The Two- and Three-Body Interaction Energy Decomposition Terms for the $NH_4^+\cdots Ar\cdots Ar$ (Figure 1c) and $NH_3\cdots Ar\cdots Ar$ (Figure 3a) Systems. Energy in kcal/mol.

n-body	$\epsilon_{el}^{(10)}$	ϵ_{ex}^{HL}	ΔE_{del}^{HF}	ΔE_{HF}	$\epsilon_{MP}^{(2)}$	ΔE_{tot}
			$NH_4^+\cdots Ar\cdots Ar$			
2	−1.058	7.495	−8.215	−1.778	−3.599	−5.376
3		0.006	0.187	0.193	0.010	0.203
tot				−1.585		−5.173
			$NH_3\cdots Ar\cdots Ar$[a]			
2	−0.328	1.189	−0.130	0.732	−1.663	−0.931
3		−0.007	0.001	−0.006	0.006	0.000
tot				0.726		−0.931

[a] Geometry of complexes from optimization based on CP-corrected potential energy surfaces.

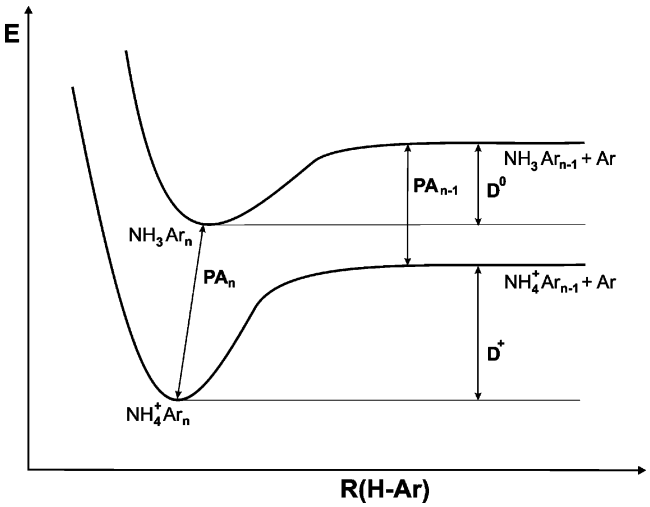

Figure 5. The schematic representation of potential energy surfaces representing the consecutive (*n* - 1, *n*) cationic and neutral complexes.

energy at the Hartree−Fock level. The Ar atoms contribute almost the same amount of electron density (0.016 electron as calculated by the NBO analysis) to the NH_4^+ core. As a consequence, the subsequent coordination of ligands significantly influences the binding properties of the core. The calculated dispersion energy ($\epsilon_{disp}^{(2)}$) matches well with the MP2 correlation energy component. Although complex cations of $NH_4^+Ar_n$ and $NH_4^+(H_2)_n$ are expected to be similar, the nature of bonding is significantly different. The argon clusters are stabilized mainly because of the dispersion energy contribution, while in molecular hydrogen complexes, the Hartree−Fock interactions prevail.[10,41]

The interactions in NH_3Ar_n moieties are very different compared to that of cationic systems. The magnitude of the interactions is smaller. The interactions are repulsive at the Hartree−Fock level, and stabilization of complexes is granted by dispersion interactions (Table 2). For Hartree−Fock interactions, the total consecutive interaction energies contain a constant component, and the variation of energy is due to the correlation contribution. The correlation contribution is mostly governed by the dispersion term. Within the solvation shell, the interaction energies are almost a linear function of the size of the cluster. The contribution of the three-body interactions is insignificant (Table 3).

C. The Properties of Proton Affinity. The proton affinity of ammonia (204 kcal/mol)[42] is reasonably reproduced by the presented calculations (Table 4). The property is perturbed by the environment due to the microsolvation reactions leading to the $NH_4^+Ar_n$ and the NH_3Ar_n complexes. The effect of microsolvation on the proton affinity is approximately additive. It is especially visible when no change in the solvation shell takes place in neutral or cationic complexes.

The schematic representation of potential surfaces for the consecutive molecular and cationic complexes (Figure 5) rationalizes the relation

$$D^+(NH_4Ar_{n-1}-Ar) - D^0(NH_3Ar_{n-1}-Ar) = PA(NH_3Ar_n) - PA(NH_3Ar_{n-1}) \quad (3)$$

where D^+ and D^0 are sequential dissociation energies of argon from charged and molecular complexes, and PA represents proton affinities. Applying eq 3 to the sequence of dissociation reactions, the difference between the solvated and bare ammonia molecule

$$\Delta PA_n = PA(NH_3Ar_n) - PA(NH_3) \quad (4)$$

can be expressed in terms of dissociation energies

$$\Delta PA_n = \sum_{i=1}^{n}\{D^+(NH_4Ar_{i-1}-Ar) - D^0(NH_3Ar_{i-1}-Ar)\} \quad (5)$$

The value of ΔPA_n may serve as a measure of the variation of proton affinity due to the order of solvation. The proton affinity is almost a linear function of the number of ligands (Figure 6). The ΔPA_n between proton affinities of consecutive complexes (eq 3) (2.22, 1.91, 1.58, and 1.46 kcal/mol) slowly decreases for the first three ligands.

The difference between the variation of consecutive proton affinities and the similar quantity calculated from total interaction energies (2.29, 1.95, 1.61, and 1.51 kcal/mol) amounts to less than 3% indicating that the proton affinity variation defined by eq 5 can be well approximated as

$$\Delta PA_n \approx -\sum_{i=1}^{n}\{\Delta E_{tot}^{+}(NH_4Ar_{i-1}-Ar) - \Delta E_{tot}^{0}(NH_3Ar_{i-1}-Ar)\} \quad (6)$$

The total interaction energies may be further expressed by contributions representing the interaction energy decomposition terms

$$\Delta PA_n = el_n + ex_n + del_n + MP2_n \quad (7)$$

TABLE 4: Consecutive Proton Affinities of NH_3Ar_n Complexes. Values in kcal/mol.

	PA_e MP2	PA_e CCSD(T)	PA_o MP2	PA_o CCSD(T)	PA Exper.	$\Delta PA_{o,n,n-1}$
NH_3	211.2	212.4	201.5	202.7	204[a]	0
NH_3Ar	214.3	216.0	204.1	205.8	206.0[b]	3.1 (2.0)[c]
NH_3Ar_2	217.1	219.3	206.5	208.7		2.9
NH_3Ar_3	219.3	220.7	208.3	209.7		1.0
NH_3Ar_4	221.6					

[a] Reference 42. [b] Experimental, calculated from thermodynamic cycle. [c] Experimental.

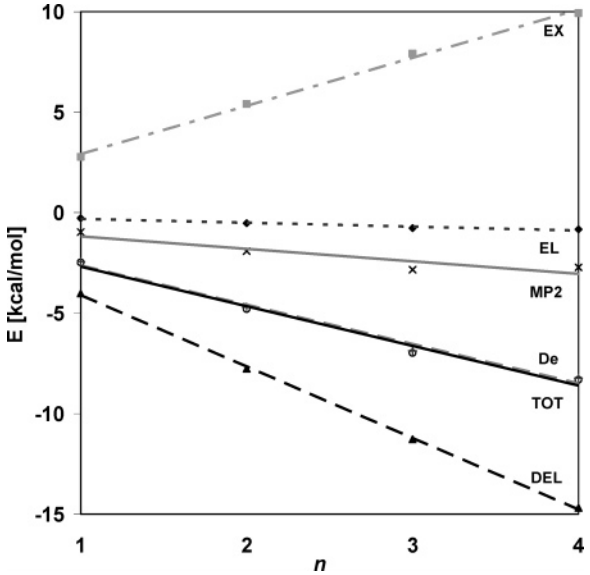

Figure 6. The contribution of interaction energy components to the variation of proton affinity of NH_3 resulting from the consecutive microsolvation by Ar atoms. D_e and tot correspond to ΔPA_n defined by the dissociation energies (D_e) and the total interaction energies (ΔE_{tot}) of the complexes, respectively (eqs 6 and 7). The el, ex, del, and MP2 contributions to the proton affinity variation are defined according to eq 8.

where the electrostatic component is defined by the equation

$$\mathrm{el}_n = -\sum_{i=1}^{n}\{\epsilon_{\mathrm{el}}^{+}(\mathrm{NH_4Ar_{i-1}} - \mathrm{Ar}) - \epsilon_{\mathrm{el}}^{0}(\mathrm{NH_3Ar_{i-1}} - \mathrm{Ar})\} \quad (8)$$

Analogous relations apply for the ex_n, del_n, and $MP2_n$ components of eq 7 which are expressed by the ϵ_{ex}^{HL}, ΔE_{del}^{HF}, and $\epsilon_{MP}^{(2)}$ terms, respectively. The results of the analysis are presented in Figure 4. All contributions are of linear character. The attractive contributions (el_n, del_n, and $MP2_n$) are dominated by the delocalization term which is balanced by the repulsive exchange interactions (ex_n).

D. The Influence of Proton Detachment on the Vibrational Frequencies of the NH_4^+ and NH_3 Cores of the Complexes. The frequencies calculated at the MP2 level were scaled to reproduce the vibrational frequency of the smallest moieties with the experimentally known fundamentals.[12,43,44] Such a procedure leads to the excellent reproduction of the available experimental results for NH_4^+Ar (Table 5). The splittings of the fundamentals due to symmetry destruction when clusters grow are well reproduced also. The calculations support the interpretation of infrared spectra of mass-selected clusters resulting from photodissociation spectroscopy.[12] More importantly, the present findings confirm earlier predictions based on the Hartree−Fock level of theory.[12]

The deprotonation of the NH_4^+ core lowers the number of vibrational modes from nine to six. Because of the degeneration imposed by the symmetry, four vibrational frequencies are observed in NH_4^+ and NH_3. All fundamentals may be observed, however, in the least symmetrical complexes. The deprotonation of $NH_4^+Ar_n$ clusters leads to a drastic change in the thermodynamics of bonding, as well asthe structural pattern is not preserved in these complexes. Upon deprotonation, the NH_4^+ characterized by the T_d structure transforms into the C_{3v} symmetry neutral ammonia. The ligands are bonded through hydrogen bonds in the cationic and neutral species, and this structural similarity allows the possible correlation between $NH_4^+Ar_n$ and NH_3Ar_n spectra to be studied. The weaker interactions in NH_3Ar_n complexes, compared to the charged species, reflects both the minor influence of microsolvation on the variation of fundamentals as well as the smaller frequency splittings. The splittings of the ν_4 fundamental in NH_3-based complexes are negligible, while the splitting of the corresponding frequency in NH_4^+ (ν_2) amounts to 13 $cm.^{-1}$ The significant splitting of the ν_3 fundamental due to the loss of the T_d symmetry of NH_4^+ is complemented by the much smaller effect of the corresponding perturbed E symmetry of NH_3.

IV. Conclusions

The gas-phase processes may be sensitive to the presence of solvent molecules even when the environment is represented by the noble gases. The proton attachment/detachment processes are vital as precursors of reactions observed in nature and are especially important for atmospheric chemistry. The formation of microclusters shapes a possible way to influence the "core" processes. The first shells of $NH_4^+Ar_n$ are formed as structures with Ar bonding via the N−H···Ar hydrogen bonds leading to

TABLE 5: MP2 Calculated Harmonic, Scaled (in square brackets), and Experimental (in parentheses) Vibrational Frequencies for $NH_4^+Ar_n$ ($n = 0-5$) Complexes. Frequencies in cm^{-1}.

n	symmetry	ν_1	ν_2	ν_3	ν_4
0	T_d	3418 (3238)	1750	3537 (3343)[a] 0.9452 s.f.[d]	1490 (1447)[b] 0.9713 s.f.[d]
1	C_{3v}	3393 3390[e] (3215)[c] 0.9475 s.f.[d]	1754 1751[e]	3545,3485 3543, 3487[e] [3351,3294] (3348,3305)	1503,1502 1496,1496[e] [1460, 1459]
2	C_{2v}	3388 (3211)	1754, 1767	3552, 3518, 3460 [3357, 3325, 3270] (3354, 3327, 3284)	1480, 1496, 1516 [1437. 1453, 1472]
3	C_{3v}	3386 [3208] (3215)	1760	3543, 3486 [3349, 3295] (3346, 3298)	1491, 1516 [1448, 1472]
4	T_d	3385 [3207]	1765	3486 [3295] (3306)	1502 [1459]
5	C_{3v}	3362 [3185] (3220)	1753	3477, 3481 [3286, 3290] (3310)	1493, 1493 [1450, 1450]

[a] Reference 43. [b] Reference 44. [c] Reference 12. [d] Scaling factor (s.f) reproducing the above experimental value. [e] Optimization on CP-corrected potential surface.

the vertex-bound structures. The second shells follow the "face" bonding path.

The subtle interactions characterizing NH_3Ar_n lead to significant problems with determining the structure of the complexes. Results of applying standard supermolecule and CP-corrected optimization schemes lead to ambiguity that is expressed by the existence of two NH_3Ar isomers, which have to be considered as possible ground states. Heavier complexes ($n > 2$) always take advantage of stabilizing Ar−Ar interactions. The studied moieties may be considered as analogues of Ar_n clusters with one atom replaced by NH_3. The molecules possess significant rotational freedom within such an arrangement.

As expected, the NH^+−Ar interactions in cationic complexes are significantly larger than NH−Ar interactions characterizing neutral complexes. The nature of the interactions in these two groups of complexes is also different. The main difference is revealed for the NH_3Ar_n species that are nonbonded at the Hartree−Fock level. The three-body interaction terms are of significant importance.

The proton affinity for consecutive complexes is a linear function of the number of ligands. More importantly, this form of the dependence also is preserved when one considers the contribution of particular terms of the interaction energy. The picture of the variation of the vibrational frequencies due to proton detachment is consistent with the trends describing the interaction energies.

Acknowledgment. This work was supported by NSF EPSCOR Grant No. 440900362427-02, CREST Grant No. HRD-01-25484, a Wroclaw University of Technology Grant, and the AHPCRC under agreement number DAAH04-95-2-00003, Contract Number DAAH04-95-C-0008, the contents of which does not necessarily reflect the position or policy of the government, and no official endorsement should be inferred. The Mississippi Center for Supercomputing Research, the Interdisciplinary Center for Mathematical and Computational Modeling of the Warsaw University, and Wroclaw Center of Computing and Networking are acknowledged for a generous allotment of computer time.

Supporting Information Available: Coordinates of structures presented in Figures 1−4. This material is available free of charge via the Internet at http://pubs.acs.org.

References and Notes

(1) Collins, M. A.; Petrie, S.; Chalk, A. J.; Radom, L. *J. Chem. Phys.* **2000**, *112*, 6625.

(2) Hiraoka, K.; Yamabe, S. *Dynamics of Excited Molecules*; Elsevier Science: Amsterdam, 1994.

(3) Bowen, K. H.; Eaton, J. G. *The Structure of Small Molecules and Ions*; Plenum: New York, 1988.

(4) Bieske, E. J.; Dopfer, O. *Chem. Rev.* **2000**, *100*, 3963.

(5) Gora, R. W.; Roszak, S.; Leszczynski, J. *J. Chem. Phys.* **2001**, *115*, 771.

(6) Gora, R. W.; Roszak, S.; Leszczynski, J. *Chem. Phys. Lett.* **2000**, *325*, 7.

(7) Read, J. P.; Buckingham, A. D. *Chem. Phys. Lett.* **1997**, *270*, 245.

(8) Meuwly, M.; Nizkorodov, S. A.; Bieske, E. J.; Maier, J. P.; Dopfer, O. *Chem. Phys. Lett.* **1997**, *270*, 252.

(9) Larkin, N. M.; Olkhov, R. V.; Dopfer, O. *Faraday Discuss.* **2001**, *118*, 455.

(10) Urban, J.; Roszak, S.; Leszczynski, J. *Chem. Phys. Lett.* **2001**, *346*, 512.

(11) Bieske, E. J.; Nizkorodov, S. A.; Dopfer, O.; Maier, J. P.; Stickland, R. J.; Cotterell, B. J.; Howard, B. J. *Chem. Phys. Lett.* **1966**, *250*, 266.

(12) Dopfer, O.; Nizkorodov, S. A.; Meuwly, M.; Bieske, E. J.; Maier, J. P. *Int. J. Mass Spectrom. Ion Processes* **1997**, *167/168*, 637.

(13) Nelson, D. D., Jr.; Fraser, G. T.; Peterson, K. I.; Zhao, K.; Klemperer, W.; Lovas, F. J.; Suenram, R. D. *J. Chem. Phys.* **1966**, *85*, 5512.

(14) Schmuttenmaer, C. A.; Loeser, J. G.; Saykally, R. J. *J. Chem. Phys.* **1994**, *101*, 139.

(15) Schmuttenmaer, C. A.; Cohen, R. C.; Saykally, R. J. *J. Chem. Phys.* **1994**, *101*, 146.

(16) Chalasinski, G.; Cybulski, S. M.; Szczesniak, M. M.; Scheiner, S. *J. Chem. Phys.* **1989**, *91*, 7809.

(17) Bulski, M.; Wormer, P. E. S.; van der Avoird, A. *J. Chem. Phys.* **1991**, *94*, 491.

(18) Møller, C.; Plesset, M. S. *Phys. Rev.* **1934**, *46*, 618.

(19) Dunning, Jr. T. H. *J. Chem. Phys.* **1989**, *90*, 1007.

(20) Kendall, R. A.; Dunning, Jr. T. H.; Harrison, R. J. *J. Chem. Phys.* **1992**, *96*, 6769.

(21) Woon, D. E.; Dunning, Jr. T. H. *J. Chem. Phys.* **1993**, *98*, 1358.

(22) Peng, C.; Ayala, P. Y.; Schlegel, H. B.; Frisch, M. J. *J. Comput. Chem.* **1966**, *17*, 49.

(23) Boys, S. F.; Bernardi, F. *Mol. Phys.* **1970**, *19*, 553.

(24) Simon, S.; Duran, M.; Dannenberg, J. J. *J. Chem. Phys.* **1996**, *105*, 11024.

(25) Kumar, A.; Meath, W. J. *Can. J. Chem.* **1985**, *63*, 1616.

(26) Herman, P. R.; LaRocque, P. E.; Stoicheff, B. P. *J. Chem. Phys.* **1988**, *89*, 4535.

(27) Bartlett, R. J.; Sekino, H.; Purvis, G. D. *Chem. Phys. Lett.* **1983**, *98*, 66.

(28) Pople, J. A.; Head-Gordon, M.; Raghavachari, K. *J. Chem. Phys.* **1987**, *87*, 5968.

(29) Davidson, N. *Statistical Mechanics*; McGraw-Hill: New York, 1962.

(30) Reed, A. E.; Weinstock, R. B.; Weinhold, F. *J. Chem. Phys.* **1985**, *83*, 735.

(31) Gutowski, M.; van Duijneveldt, F. B.; Chalasinski, G.; Piela, L. *Mol. Phys.* **1987**, *61*, 233.

(32) Sokalski, W. A.; Roszak, S.; Pecul, K. *Chem. Phys. Lett.* **1988**, *153*, 153.

(33) Cybulski, S. M.; Chałasiński, G.; Moszyński, R. *J. Chem. Phys.* **1990**, *92*, 4357.

(34) Jansen, H. B.; Ros, P. *Chem. Phys. Lett.* **1969**, *3*, 140.

(35) Frisch, M. J.; Trucks, G. W.; Schlegel, H. B.; Scuseria, G. E.; Robb, M. A.; Cheeseman, J. R.; Montgomery, J. A., Jr.; Vreven, T.; Kudin, K. N.; Burant, J. C.; Millam, J. M.; Iyengar, S. S.; Tomasi, J.; Barone, V.; Mennucci, B.; Cossi, M.; Scalmani, G.; Rega, N.; Petersson, G. A.; Nakatsuji, H.; Hada, M.; Ehara, M.; Toyota, K.; Fukuda, R.; Hasegawa, J.; Ishida, M.; Nakajima, T.; Honda, Y.; Kitao, O.; Nakai, H.; Klene, M.; Li, X.; Knox, J. E.; Hratchian, H. P.; Cross, J. B.; Bakken, V.; Adamo, C.; Jaramillo, J.; Gomperts, R.; Stratmann, R. E.; Yazyev, O.; Austin, A. J.; Cammi, R.; Pomelli, C.; Ochterski, J. W.; Ayala, P. Y.; Morokuma, K.; Voth, G. A.; Salvador, P.; Dannenberg, J. J.; Zakrzewski, V. G.; Dapprich, S.; Daniels, A. D.; Strain, M. C.; Farkas, O.; Malick, D. K.; Rabuck, A. D.; Raghavachari, K.; Foresman, J. B.; Ortiz, J. V.; Cui, Q.; Baboul, A. G.; Clifford, S.; Cioslowski, J.; Stefanov, B. B.; Liu, G.; Liashenko, A.; Piskorz, P.; Komaromi, I.; Martin, R. L.; Fox, D. J.; Keith, T.; Al-Laham, M. A.; Peng, C. Y.; Nanayakkara, A.; Challacombe, M.; Gill, P. M. W.; Johnson, B.; Chen, W.; Wong, M. W.; Gonzalez, C.; Pople, J. A. *Gaussian 03*, revision C.02; Gaussian: Pittsburgh, PA, 2004.

(36) Gora, R. W. *EDS*, v2.1.2 package; Wroclaw, Poland, and Jackson, MS, USA (1998−2004).

(37) Schmidt, M. S.; Baldridge, K. K.; Boatz, J. A.; Elbert, S. T.; Gordon, M. S.; Jensen, J. H.; Koseki, S.; Matsunaga, N.; Nguyen, K. A.; Su, S. J.; Windus, T. L.; Dupuis, M.; Montgomery, J. A. *J. Comput. Chem.* **1993**, *14*, 1347.

(38) Hobza, P.; Bludsky, O., Suhai, S. *Phys. Chem. Chem. Phys.* **1999**, *1*, 3073.

(39) Dopfer, O.; Nizkorodov, S. A.; Meuwly, M.; Bieske, E. J.; Maier, J. P. *Chem. Phys. Lett.* **1996**, *260*, 545.

(40) Chalasinski, G.; Szczesniak, M. M.; Cybulski, S. M. *J. Chem. Phys.* **1990**, *92*, 2481.

(41) Szymczak, J. J.; Grabowski, S. J.; Roszak. S.; Leszczynski, J. *Chem. Phys. Lett* **2004**, *393*, 81.

(42) Hunter, E. P.; Lias, S. G. *J. Phys. Chem. Ref. Data* **1998**, *27*, 413.

(43) Schäfer, E.; Saykally, R. J.; Robiette, A. G. *J. Chem. Phys.* **1984**, *80*, 3969.

(44) Polak, M.; Gruebele, M.; DeKock, B. W.; Saykally, R. J. *Mol. Phys.* **1989**, *66*, 1193.